Neuron, Vol. 30, 593–607, May, 2001, Copyright ©2001 by Cell Press

Neuronal Correlates of Motor Performance and Motor Learning in the Primary Motor Cortex of Monkeys Adapting to an External Force Field

Chiang-Shan Ray Li,[1,3] Camillo Padoa-Schioppa,[1] and Emilio Bizzi[1,2]
[1]Department of Brain and Cognitive Sciences
Massachusetts Institute of Technology
Cambridge, Massachusetts 02139

Summary

The primary motor cortex (M1) is known to control motor performance. Recent findings have also implicated M1 in motor learning, as neurons in this area show learning-related plasticity. In the present study, we analyzed the neuronal activity recorded in M1 in a force field adaptation task. Our goal was to investigate the neuronal reorganization across behavioral epochs (before, during, and after adaptation). Here we report two main findings. First, memory cells were present in two classes. With respect to the changes of preferred direction (Pd), these two classes complemented each other after readaptation. Second, for the entire neuronal population, the shift of Pd matched the shift observed for muscles. These results provide a framework whereby the activity of distinct neuronal subpopulations combines to subserve both functions of motor performance and motor learning.

Introduction

A wealth of evidence derived from studies with humans and nonhuman primates indicates that the sensory and motor areas of the cerebral cortex are plastic. For instance, experiments on primates showed that re-mapping occurs in the somatosensory cortex when sensory nerves from a body part are severed or deactivated by a local anesthetic (Faggin et al., 1997; Florence and Kaas, 1995; Manger et al., 1996; Borsook et al., 1998). After recovery, the cortical area deprived of the sensory input from the amputated part was activated by stimulation of an adjacent body part. Similar observations have been made when a lesion was selectively placed in a small, circumscribed cortical area (Xerri et al., 1998). Neuronal plasticity has also been demonstrated in studies employing electrical microstimulation and behavioral training. For instance, it was found that cortical representation increases in the primary auditory cortex for a frequency range that monkeys were trained to discriminate (Recanzone et al., 1993). Nudo and colleagues used intracortical microstimulation to map the representation of the distal forelimb zone of the primary motor cortex of monkeys (Nudo et al., 1996). Microstimulations were applied before and after training on two tasks that differentially engaged specific sets of digit and forelimb movements. When monkeys performed in a small object retrieval task, in which they actively used their digits, the cortical representation of their digits increased. In contrast, when monkeys were trained on a key-turning task, which engaged the wrist/forearm, the corresponding cortical areas were found to be enlarged.

Further evidence for plasticity comes from functional imaging experiments with humans. Studies using magnetic source imaging revealed that the cortical representation of the left-hand digits of string players was larger than that of control subjects (Elbert et al., 1995). Training on a sequence of finger movements over a few weeks resulted in enlarged activation of the primary motor cortex when subjects performed the practiced sequence, compared to a novel, unpracticed sequence (Karni et al., 1995). Using transcranial magnetic stimulation (TMS), Pascual-Leone and colleagues found that both mental and physical practice led to an improvement in five-finger piano exercises. Such improvement was associated with the modulation of cortical motor output to the muscles utilized in the task (Pascual-Leone et al., 1994). More recently, Classen and colleagues used focal TMS of the motor cortex to elicit isolated limb movements (Classen et al., 1998). They found that continuous training on a particular direction of thumb movement for as little as 10 min could bias the direction of evoked movements, suggesting that training rapidly alters the cortical network subserving thumb movement. The authors speculated that this change could subserve a short-term memory for movement and might potentially be the first stage of skill acquisition.

Neuronal recordings from awake, behaving monkeys have also revealed plasticity at the single cell level in a number of learning tasks. For example, neurons in the primary motor cortex, the premotor cortex, and the supplementary eye field exhibited learning-dependent activity changes in a visuomotor association task (Mitz et al., 1991; Chen and Wise, 1995; Wise et al., 1998). Nakamura and colleagues showed that a subset of medial frontal neurons were more active during performance of a new sequence compared to a learned sequence of movements, and suggested that these neurons might be involved in the acquisition of new sequential procedures (Nakamura et al., 1998). Previous studies on the neural correlates of long-term memory had also revealed neuronal plasticity associated with perceptual learning (Sakai and Miyashita, 1991).

To our knowledge, however, no studies have explored changes in neuronal activity during learning that involved a change in movement dynamics. Psychophysical experiments conducted in our laboratory have demonstrated that human subjects adapt to a viscous force field imposed on their visually guided planar reaching movements (Shadmehr and Mussa-Ivaldi, 1994). The perturbation of the movement trajectories decreased and eventually disappeared as subjects adapted to these force fields. When the force field was removed, the movement trajectories curved in the direction opposite of that observed when the force field was first imposed. The existence of this aftereffect suggested that subjects developed an internal model of the dynamics of the motor environment as they adapted to the force field. In the current study, we extended the force field adaptation paradigm to monkeys. Our aim was to examine the change in neuronal activity in the primary motor

[2]Correspondence: emilio@ai.mit.edu
[3]Present address: Departments of Psychiatry/Physiology, Chang Gung Memorial Hospital and Chang Gung University, Kwei-shan, Tao-yuan 333, Taiwan.

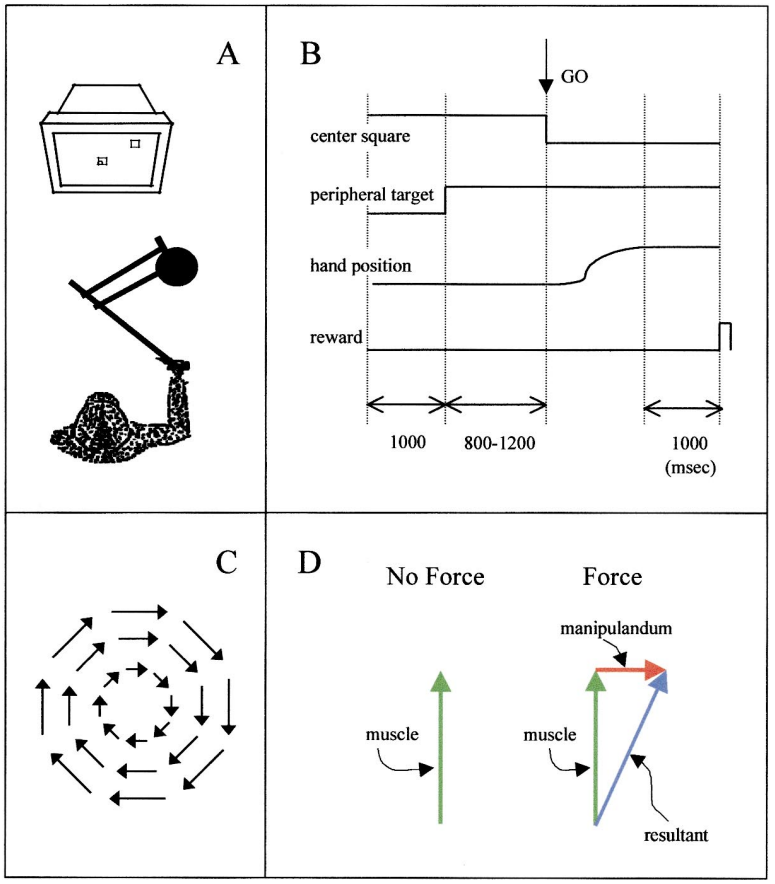

Figure 1. The Experimental Setup and the Behavioral Paradigm

(A) The monkey held a two-link low-friction manipulandum. Two torque motors mounted at the base of the manipulandum and connected independently to each joint enabled specific forces to be applied.

(B) The trial structure of the delayed, visually instructed, reaching task (see text).

(C) The clockwise curl force field used in the experiment is plotted in velocity space. The direction of the perturbing force is orthogonal to the hand velocity and the magnitude proportional to the hand speed.

(D) Predictions of change in the preferred direction (Pd) of muscles' EMG during exposure to a curl field. In the absence of external forces (left), only muscles (green) exert a force upon the hand of the monkey. When a clockwise force field is introduced (right), two forces are present: the force exerted by the muscles (green) and the force exerted by the manipulandum (red). The vector sum of these two forces gives a resultant force (blue) pointing in a direction shifted clockwise. The Pd of each muscle, represented in real space, shifts in the Force epoch compared to the Baseline. For all muscles, this shift occurs in the same direction, namely the direction of the external force. When the force is turned off, the Pd of each muscle returns to its original value.

cortex of monkeys as they adapt to a new dynamic environment.

We have previously reported that when monkeys engage in this adaptation paradigm, new cells (tune-in cells) are recruited as other cells leave the pool (tune-out cells) (Gandolfo et al., 2000). In the present study, we investigated the changes of the neuronal activity of the primary motor cortex (M1) with respect to the parameters characterizing their tuning curves. We found that two different classes of memory cells coexist and balance each other after exposure to the force field. When the entire population was considered, the changes of preferred direction across behavioral epochs observed for neurons matched the corresponding changes observed for muscles. This match was due to the concurrent presence of the two classes of memory cells.

Results

Adaptation to the Force Field

Two monkeys performed center-out visually instructed reaching movements. The monkeys held the manipulandum of a two-degree-of-freedom, lightweight, low-friction robot arm. The position of the manipulandum and the targets were displayed on a computer monitor placed in front of the monkey (Figure 1A). This setup was essentially identical to that previously used in human behavioral studies (Shadmehr and Mussa-Ivaldi, 1994). In the task, the monkeys performed delayed, visually instructed, reaching movements, as illustrated in Figure 1B. Each experimental session was divided into three behavioral epochs: (1) a Baseline epoch, in which the monkey performed the task without a force field; (2) a Force epoch, in which a force field was applied; and (3) a Washout epoch, in which the force field was removed. Typically, the monkey performed 160 to 200 successful trials ("hits") in each epoch, which averaged to 20 to 25 "hits" for each of the eight movement directions. Each experiment lasted for approximately 2 hr. In each session, one of two curl, viscous force fields—clockwise or counterclockwise—was applied in the Force epoch (Figure 1C). These force fields imposed predictable changes on the muscular activity in the Force epoch (Figure 1D).

To characterize the "goodness" of movements, we derived the speed profile from each trajectory. We then computed a correlation coefficient (CC) measuring the similarity between the actual speed profile and an ideal speed profile (Shadmehr and Mussa-Ivaldi, 1994). The values of the CC range between −1 and 1, and are close to 1 when the actual speed profiles are close to ideal. The results of a representative experimental session are depicted in Figure 2. In the Baseline, when no force was present, the CC was high and the trajectories were straight. When a counterclockwise force field was introduced, the performance deteriorated (the CC dropped) and trajectories deviated in the direction of the force. As the monkey adapted to the perturbation, however, trajectories returned straight and the CC reached a steady state. During the late Force epoch, the performance was essentially indistinguishable from the Baseline. When the force field was removed, in the Washout,

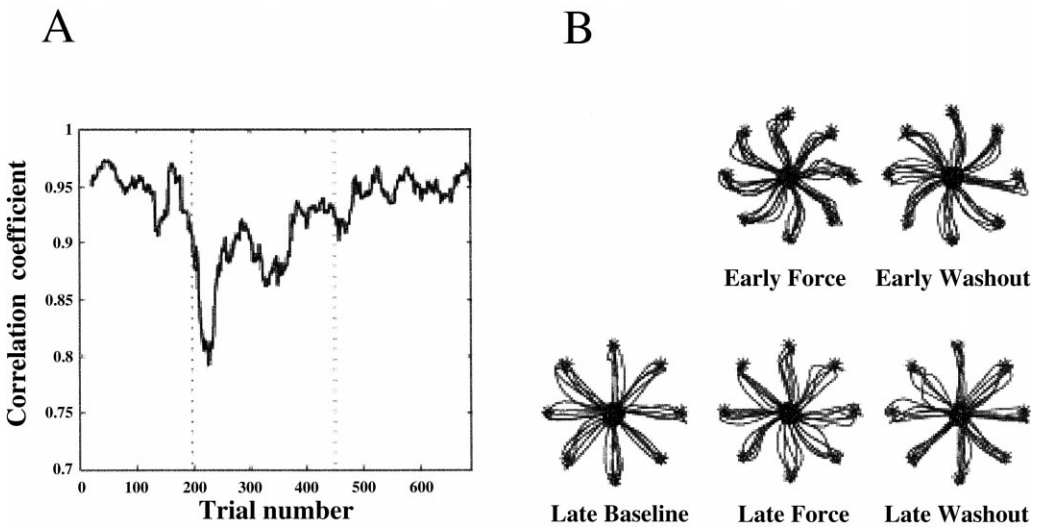

Figure 2. Correlation Coefficient and Movement Trajectories in the Three Behavioral Epochs

(A) The correlation coefficient (CC) was close to 1 in the Baseline (performance close to ideal). In the Force epoch, the CC dropped abruptly and gradually recovered, reaching a steady state. In the Washout, the CC briefly decreased again (aftereffect), and then quickly returned to the original levels.

(B) Trajectories recorded in the same day. Note that the deviations observed in the aftereffect mirror the early effects of the force field.

an "aftereffect" was observed in which the trajectories deviated in a way that mirrored the change in the early Force. After a brief readaptation phase, the movement trajectories again became straight and the CC regained its original high values.

The activity of neurons in the primary motor cortex (M1) was recorded while monkeys performed during the Baseline, Force, and Washout epochs. In the analysis presented in the following sections, we focused on the neuronal and muscular activity recorded in trials with similar kinematics. In other words, we only considered trials corresponding to the three bottom panels of Figure 2B and to the steady-state regions of the correlation coefficient. Thus, we were able to dissociate the neural activity related to the kinematics from the activity related to the dynamics of movement. In the Force epoch, the kinematics were essentially the same as in the Baseline (i.e., the trajectories were straight and the speed profiles were close to ideal). However, the dynamics were different since the monkeys compensated for the external force field in the Force epoch but not in the Baseline. In addition, we were able to dissociate the motor performance from the effects of motor adaptation. In the Washout, the performance of the monkeys was essentially identical to the Baseline, both in terms of the kinematics and the dynamics of movement. Differences in activity between the Washout and the Baseline epochs were therefore attributed to the effects of adaptation. These considerations served as the basis for classifying neurons.

Neural Plasticity in M1

A total of 162 neurons were considered for the present analysis. For each trial, we analyzed the neuronal activity from 200 ms before the onset of the movement to the end of the movement (movement-related activity). A tuning curve was constructed from the neuronal activity of the eight directions of movement. Three parameters were used to characterize each tuning curve. (1) The preferred direction (Pd) was defined as the direction of the vector sum of the vectors representing the activity for each of the eight directions of movement. (2) The average firing frequency (Avf) was defined as the average of the neuronal firing rates in the eight movement directions. (3) The tuning width (Tw) was defined as the angle over which the activity was higher than half of the maximal activity (maximum of the tuning curve). The Pd and Tw were computed only for those neurons showing a significant nonuniform distribution of activity across the eight movement directions ($pR < 0.05$, Rayleigh test). The neuronal activity in the Baseline, Force, and Washout epochs were statistically compared in terms of the three parameters used to characterize the tuning curve. The comparison was made separately for each parameter.

Neurons whose activity remained invariant across the three behavioral epochs (*x-x-x*) were called kinematic cells, as their activity appeared to be correlated with the kinematics of the movement. Neurons whose activity was modulated by the force field (*x-y-x*) were called dynamic cells. Some cells, modulated by the force field, retained their modulation in the Washout epoch such that their activity profile in the Washout was more similar to that in the Force than in the Baseline epoch (*x-y-y*). These neurons were named "memory" cells, as they appeared to maintain in the Washout a memory trace of the force field imposed in the Force epoch. We also found another class of cells whose activity was not modulated by the force but was modulated in the Washout (*x-x-y*). We classified the (*x-x-y*) cells as memory cells because their activity in the Washout was different from the Baseline. We named the (*x-y-y*) and (*x-x-y*) cells Class I and Class II memory cells, respectively. In some instances, cells were modulated by the force and again in the Washout (*x-y-z*).

Figures 3A–3E show examples of kinematic, dynamic, and memory cells. Since the preferred direction (Pd), average firing frequency (Avf), and tuning width (Tw) were used separately to characterize the neuronal activ-

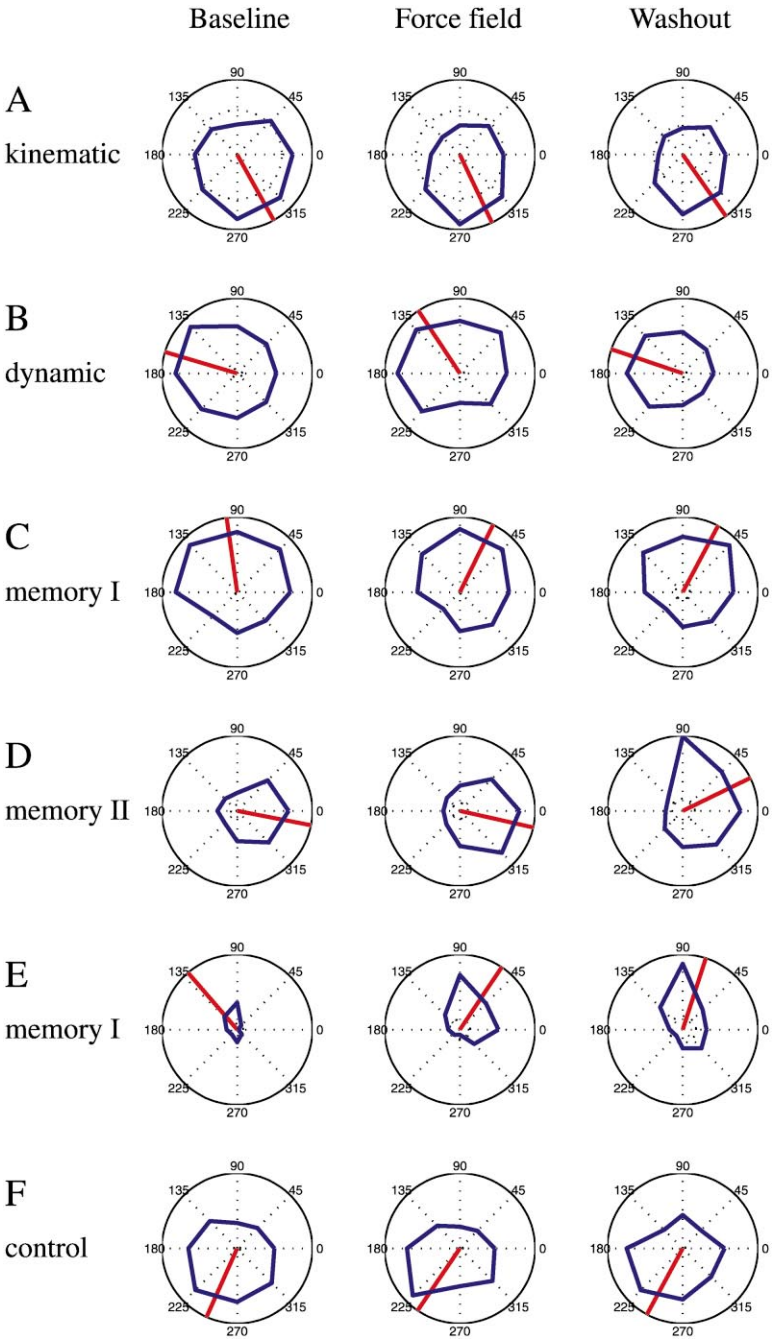

Figure 3. Examples of Cells

The tuning curves are plotted in polar coordinates. For each cell, the three plots represent the movement-related activity in the Baseline (left), in the Force epoch (center), and in the Washout (right). In each plot, the circle in dashed line represents the average activity during the center hold time window, when the monkey holds the manipulandum inside the center square and waits for instructions. (A), (B), (C), and (D) are examples of kinematic (*x-x-x*), dynamic (*x-y-x*), memory I (*x-y-y*), and memory II (*x-x-y*) cells, in terms of the modulation of the Pd. A neuron could display modulation in more than one parameter. For instance, the neuron shown in (B) has dynamic property both in terms of the Pd and the Tw, and (E) shows a neuron that has memory property both in terms of the Avf and the Pd. (F) shows a neuron collected in a control experiment, in which no force field was used. The Pd remained unchanged across the three arbitrarily divided behavioral epochs, each consisting of 200 successful trials. All cells (A)–(E) were recorded with a clockwise force field. Cells (A)–(C) are from monkey B, cells (D)–(F) are from monkey M. All plots are normalized to the maximal activity across the three epochs. The labels on the left refer to the changes of Pd.

ity, a cell could exhibit dynamic or memory properties in terms of any of the three parameters. The shifts of Pd are particularly interesting because they reflect the constraints imposed by the curl force fields. The Pd of the cell shown in Figure 3A remained essentially unchanged across the three behavioral epochs. This cell was thus classified as kinematic. Dynamic cells shifted their Pd in the Force epoch compared to the Baseline. This shift typically occurred in the direction of the applied force field (clockwise in the example shown in Figure 3B). In the Washout, the Pd of dynamic cells returned to their original values. Class I memory cells (*x-x-y*) shifted their Pd in the Force epoch. Their shifts also occurred in the direction of the external force field (Figure 3C). In the Washout, however, Class I memory cells maintained their newly acquired Pd. In contrast, Class II memory cells (*x-y-y*) did not change their Pd in the Force epoch, but shifted their Pd in the Washout. This shift typically occurred in the direction opposite to the previously experienced force field. For the cell shown in Figure 3D, which was recorded in a session where a clockwise force field had been introduced in the Force epoch, the shift of Pd occurred in the Washout in the counterclockwise direction.

Recording experiments were occasionally conducted without using the force field (seven cells total). In these sessions, the monkeys performed approximately 600 hits in the Baseline condition. Three cells were direction-

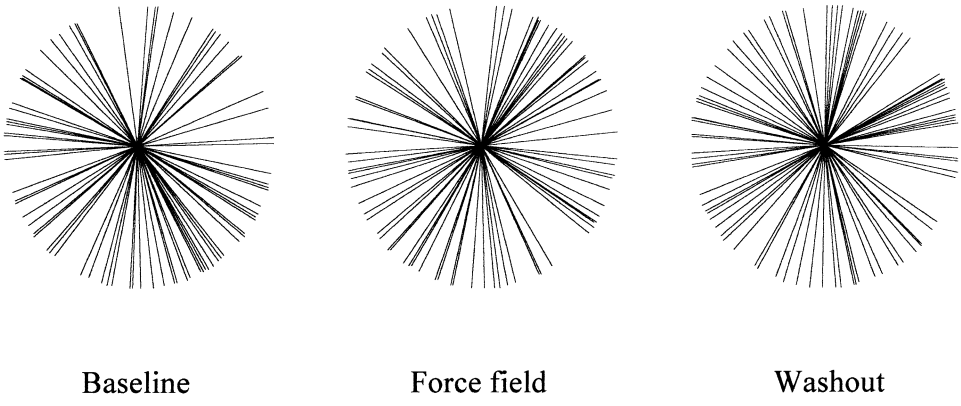

Figure 4. Distribution of the Preferred Directions

Each line represents the Pd of a single neuron. Circular statistics showed that the distribution is homogeneous across directions in all three epochs (see text).

ally tuned in all three epochs and all of them were classified as kinematic according to the changes of Pd. Figure 3F shows one cell recorded in a control experiment. It can be seen that the tuning curve stays essentially stable throughout the session.

At the population level, we first analyzed the distribution of the preferred directions. The distribution for the three behavioral epochs is shown in Figure 4. Circular statistics performed to test for the homogeneity of the distribution revealed that the null hypothesis of homogeneity holds for all three epochs ($V = 1.279$, Baseline; $V = 0.838$, Force; $V = 1.236$, Washout; $p > 0.15$ in all cases; see Fisher, 1993). We then studied the shifts of Pd across epochs. As a population, the neurons showed a shift of Pd in the direction of the applied force field in the Force epoch compared to the Baseline (average change of Pd = 16.2°, SD = 26°, $p < 10^{-6}$, Figure 5A). As the monkey continued in the Washout epoch, the Pd shifted in the opposite direction (14.3°, SD = 32°, $p < 0.0003$), such that there was no net change of Pd between the Washout and the Baseline ($p = 0.9$). The fact that the changes of Pd between the Washout and the Baseline essentially averaged to zero reflects the presence of the two classes of memory cells. Furthermore, at the population level, the neuronal shifts of Pd across epochs matched the shifts of Pd recorded for single muscles (see next section).

We also studied the differences of average firing frequency (Avf) between the Force epoch and the Baseline for the neuronal population (Figure 5B). The Avf increased in the Force epoch compared to the Baseline, and the average increase was 19% (SD = 65%, $p < 0.001$). The Avf increased again by 12% (SD = 51%, $p < 0.004$) in the Washout, compared to the Force epoch.

Finally, we analyzed the changes of tuning width (Tw) across epochs. As a population, neurons did not show any significant change of Tw in the Force epoch or in the Washout (Figure 5C).

Figure 6 shows, for each parameter, the change in the Force epoch compared to the Baseline versus that in the Washout compared to the Force epoch. All neurons are shown and color coded according to their category. Consider first the three plots 6Aa, 6Bb, and 6Cc (diagonal plots), referring to the changes of Pd, Avf, and Tw, respectively. The kinematic cells (black) show no significant change in either x or y measures, and lie close to the origin of the axes. The dynamic cells (blue) show changes on both axes, but in opposite directions, and thus lie on the diagonal crossing the second and fourth quadrant. The Class I memory cells (green) display modulation in the x but not in the y measure and therefore lie close to the *x* axis. The Class II memory cells (red), displaying a modulation in the y but not in the x measure, lie on the *y* axis. Note that there do not appear to be clear-cut boundaries between the different categories of neurons, which were classified according to statistical measures. The percentages of cells in each category, for the three parameters studied, are reported in Table 1.

The other, off-diagonal plots of Figure 6 illustrate the relations between changes of different parameters. Consider for instance plot 6Ab. The position of each cell in the plot refers to the changes of Pd (axes: Pd), while the color refers to the changes of Avf (color: Avf). The conventions for colors are the same as in the diagonal plots. It can be seen that, unlike in the diagonal plots, there is no systematic relationship between the color and the position on the axes. In other words, the classifications performed according to the Pd and the Avf appear to be independent. The same conclusion holds when considering plot 6Ba, where the position on the axes refers to the changes of Avf (axes: Avf) and the color refers to the changes of Pd (color: Pd). The remaining plots illustrate the relations between changes of Pd and changes of Tw (plots 6Ac and 6Ca) and between changes of Avf and changes of Tw (plots 6Bc and 6Cb). Again, the classifications based upon different parameters do not appear to be directly related.

Finally, when multiple parameters were considered at the same time, most neurons showed some change across epochs (61/64 considering Pd and Avf; 21/25 considering Pd and Tw; 24/25 considering Avf and Tw; 25/25 considering Pd, Avf, and Tw).

Electromyographic Activity: Theoretical Predictions and Experimental Results

The electromyographic activity (EMG) was rectified and integrated over the same movement-related time window used for cells (from 200 ms before movement onset

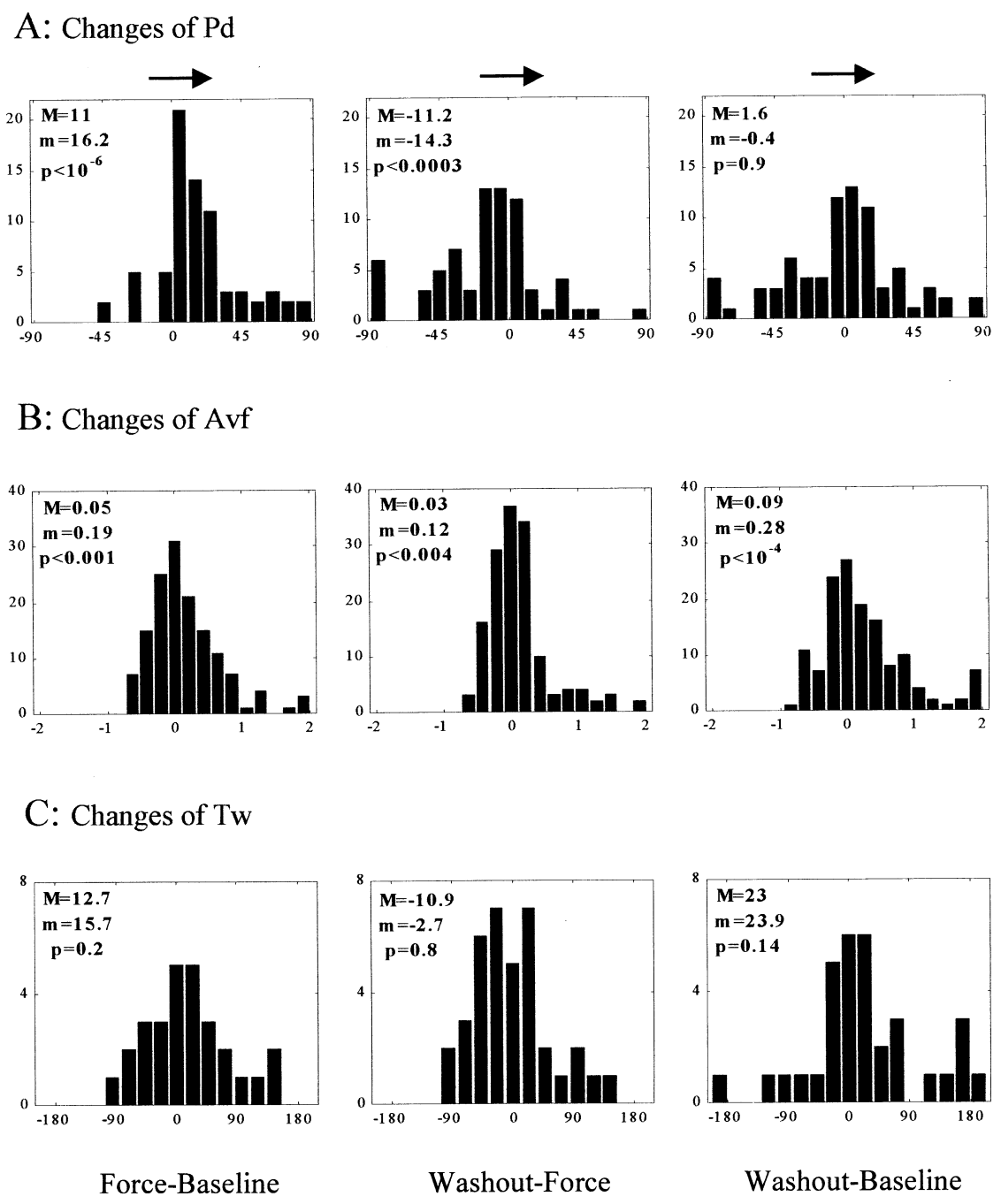

Figure 5. Histograms

Changes in the preferred direction (A), average firing frequency (B), and tuning width (C) for the activity of M1 neurons as a population during the movement-related time period in the force adaptation task. The arrows in (A) indicate the direction of the force field. The preferred directions are "flipped" for cells recorded with the CK force field. The plots in the first column represent the difference between the Force and Baseline epochs, the second column the difference between the Washout and Force epochs, and the third column the difference between the Washout and Baseline epochs. The vertical axis represents the number of cells. In each plot, M is the median of the histogram, m is the mean of the histogram, and p is the p value obtained from a t test (circular t test for Pd and Tw).

up to the end of movement). We represented the activity of each muscle with a tuning curve and defined a preferred direction. The curl fields used in the adaptation paradigm provided an isotropic (rotation-invariant) perturbation, in that the external force was always orthogonal to the movement for all eight directions. This choice imposed a constraint on the change in muscle activity following adaptation to the force field (Figure 1D). Briefly, when monkeys performed in the Force epoch, the external force summed with the force exerted by the muscles on the hand. As a result, the preferred direction of the muscles rotated in the direction of the external force

field. Because the perturbation was isotropic, the rotation occurred for all muscles in the same direction—clockwise or counterclockwise depending on the force field used—irrespective of their initial preferred direction.

These predictions were experimentally confirmed. For muscles, the directional tuning of the EMG activity changed in the direction of the applied force in the Force epoch and returned to the baseline in the Washout epoch. Figure 7 shows the EMG data collected from four muscles recorded with a clockwise force field. The data are plotted separately for each muscle sampled and for each behavioral epoch. We observed that the preferred direction of all four muscles rotated in the direction of the force in the Force epoch, and rotated back in the Washout. On average, the Pd of muscles shifted by 18.8° (median 21.4°) in the Force epoch compared to the Baseline, and shifted back by −21.7° (median −21.7°) in the Washout compared to the Force epoch. The classification of muscles is reported in Table 2.

Discussion

Single Cell Plasticity and Population Changes in the Primary Motor Cortex

If the primary motor cortex ultimately controls the movement through its projections to the subcortical structures and the spinal cord, then its overall output should be the same in the Washout and in the Baseline. In other words, in order to subserve the function of *motor performance*, the neuronal population of M1 must transmit analogous commands before and after the adaptation experience. On the other hand, this and other studies provide evidence for neural plasticity in M1 associated with motor learning. In the present study, we show that plastic changes in memory cells outlast the exposure to the force field, reflecting the development of an internal model. These findings suggest that M1 is also involved in *motor learning*. But how can these two functions, of motor performance and motor learning, be achieved by the same neuronal population? Two findings reported here are relevant to this issue. First, two classes of memory cells were found. With regard to the change of preferred direction, these two classes balanced each other in the Washout. Second, when the entire neuronal population was considered, the changes of preferred direction matched the changes observed for muscles. Taken together, these findings suggest that while single neurons change their activity when a new internal model is developed (motor learning), the entire neuronal population reorganizes itself to transmit a signal appropriate for the behavioral goal (motor performance).

The curl force fields used in this experiment imposed a constraint on the effects of adaptation on muscular activity. In accord with the predictions illustrated in Figure 1D, the preferred direction (Pd) of muscles rotated in the direction of the external force in the Force epoch and rotated back in the Washout epoch. Incidentally, this confirms previous results from a study on humans performing an identical learning task (Thoroughman and Shadmehr, 1999). For neurons, we found several classes of cells, including memory cells that have different Pd in the Washout compared to the Baseline. Thus, *single cells* did not simply reflect the changes of muscle activity. The *neuronal population*, however, matched the changes observed for muscles. As a population, the Pd of neurons shifted in the direction of the applied force in the Force epoch and shifted back in the opposite direction in the Washout epoch. The magnitude of the Pd shift of the neuronal population (16.2° Force-Baseline; −14.3° Washout-Force) was smaller, though comparable, to that observed for muscles (18.8° Force-Baseline; −21.7° Washout-Force).

The match between the neuronal population and the muscle activity could be accounted for by the presence of both Class I and Class II memory cells. On the one hand, Class I memory cells (*x-y-y*) typically shifted their Pd in the direction of the force field in the Force epoch and retained this shift in the Washout epoch. On the other hand, Class II memory cells (*x-x-y*) did not change their Pd in the Force epoch. Their Pd, however, shifted in the Washout epoch in the direction *opposite* to the previous force field. In the Washout epoch, the shifts of Pd of the Class I and Class II memory cells balanced each other. As a result, for the neuronal population, the changes of Pd between the Washout and the Baseline essentially averaged to zero. Notably, the percentages of the Class I and Class II memory cells were similar (19% versus 22%).

In our interpretation, Class I and Class II memory cells are complementary correlates of motor performance and motor learning. After readaptation in the nonperturbed condition (Washout), the neuronal population returns to a state statistically indistinguishable from the initial state (Baseline). Correspondingly, the motor performance, as dictated by the activity of the neuronal population, assumes similar values in terms of both the kinematics and the dynamics of movements. At the single cell level, however, the activity of neurons after readaptation still reflects the previous adaptation to the force field. Such plasticity parallels the development of an internal model of the dynamic environment.

Neuronal Plasticity and Short- versus Long-Term Motor Learning

In the present study, we used the correlation coefficient (CC) as an indicator of behavioral performance. From a psychophysical standpoint, the observation of the CC revealed several stages of motor learning. First, within each session, the CC increased across trials in the Force epoch, as illustrated in Figure 2A. We refer to this stage as motor adaptation, or short-term learning. Second, we computed the mean CC in the Force epoch for each session (i.e., for each day) and studied its trend across sessions. The mean CC increased, and reached a plateau within 15–25 sessions in the same force field (data not shown). Third, for both monkeys, the mean CC reached a plateau within fewer sessions for the second force field than for the first force field (6–8 days for the second field versus 15–25 days for the first field) (C. Padoa-Schioppa et al., 1998, Soc. Neurosci., abstract). We refer to these last two stages as long-term learning. Interestingly, these stages closely parallel those obtained in previous reports on the learning of motor sequences (Hikosaka et al., 2000).

The present study investigated the neural correlates of motor adaptation. Independently of its significance for long-term learning, the neuronal plasticity observed here occurred within a single session. In this respect, it should be more precisely referred to as short-term plasticity. Previous studies have demonstrated that indi-

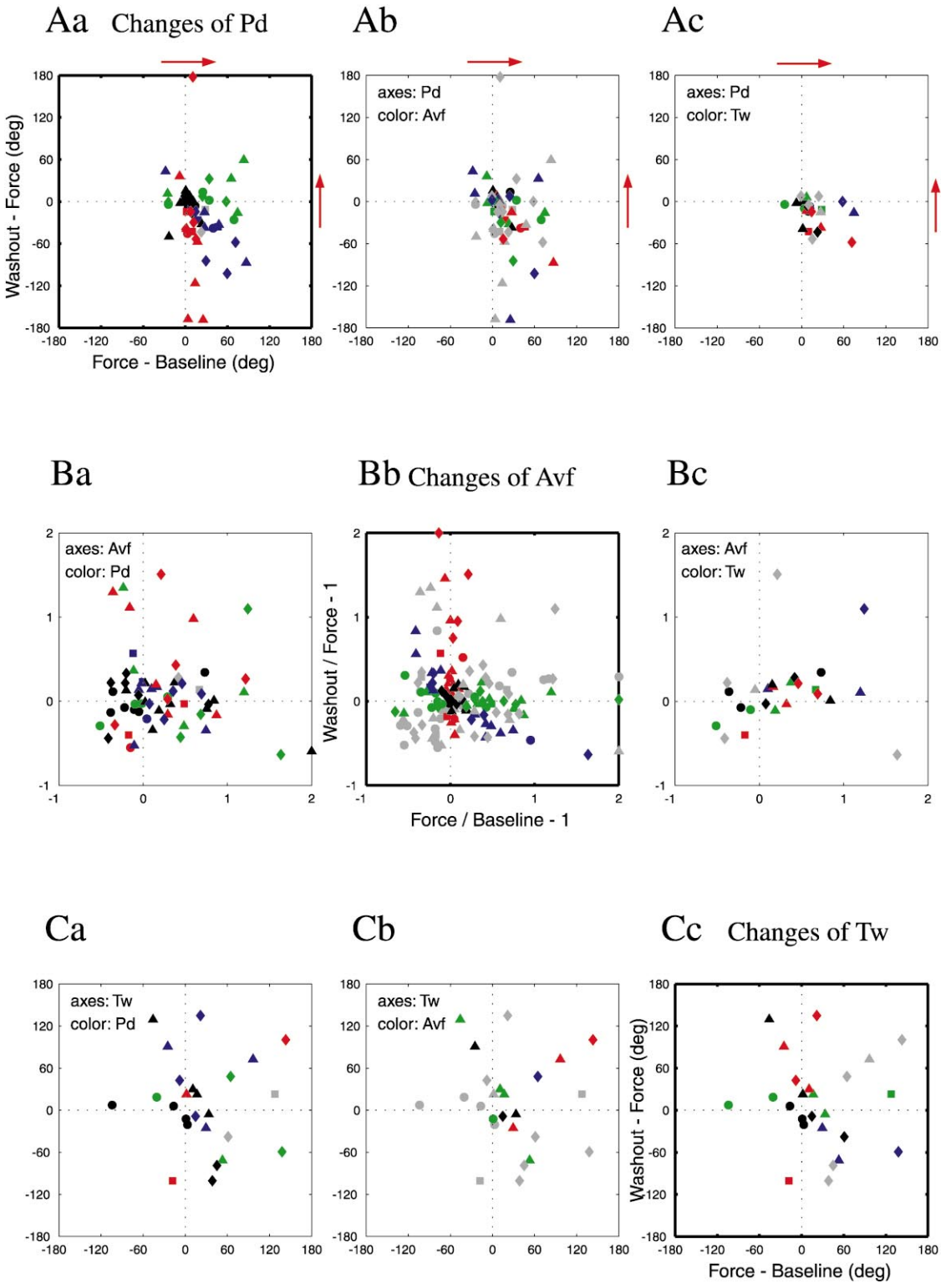

Figure 6. Scatter Plots

Diagonal plots. Cells were separately classified according to the changes of Pd (Aa, top left), the changes of Avf (Bb, center), and the changes of Tw (Cc, bottom right). In each plot, the *x* axis represents the change in the measure in the Force epoch compared to the Baseline, and the *y* axis represents the change in the Washout compared to the Force epoch. The kinematic cells (black) do not show any significant change either for the x or the y measure and are close to the origin. The dynamic cells (blue) show a change in the Force epoch compared to the Baseline, and the opposite effect in the Washout compared to the Force epoch. These cells lie on the diagonal over the second and fourth quadrant. The "*x-y-y*" cells (or memory I cells) are represented in green. These cells show a significant change between the Force epoch and the Baseline, but not between the Washout and the Force epoch. Thus, they lie on the *x* axis. The "*x-x-y*" cells (or memory II cells) are

Table 1. Classification of Cells Recorded in the Force Field Adaptation Task

	Preferred Direction	Average Firing Rate	Tuning Width
Kinematic (*x-x-x*)	22 (34%)	13 (9%)	7 (28%)
Dynamic (*x-y-x*)	14 (22%)	18 (13%)	3 (12%)
Memory I (*x-y-y*)	12 (19%)	29 (21%)	5 (20%)
Memory II (*x-x-y*)	14 (22%)	22 (16%)	5 (20%)
Other (*x-y-z*)	2 (3%)	55 (40%)	5 (20%)
Total	64 (100%)	137 (100%)	25 (100%)

vidual neurons can reflect the acquisition of a conditioned response within several minutes of sensorimotor associations (Mitz et al., 1991; Aosaki et al., 1994; Chen and Wise, 1995; Wise et al., 1998). A recent experiment revealed neuronal activity underlying rapid motor adaptation in the superior colliculus, concordant with progressively shorter reaction times (Dorris et al., 2000). Overall, a growing body of evidence supports the idea that neuronal plasticity can occur over a very short period of time. Mechanisms previously proposed in a number of studies, such as the unmasking of preexisting horizontal synaptic connections, could account for the plasticity observed here together with its time scale (Donoghue, 1995; Hess et al., 1996; Dinse et al., 1997; Huntley, 1997; Laubach et al., 2000).

The data reported here were collected starting from the first day the monkeys were exposed to the force fields up to sessions well within the long-term learning plateau. Different classes of cells, including memory cells, were recorded in all phases of the long-term learning curve, and sometimes in the same session. Although we cannot conclude from the present data that the neuronal plasticity observed here is directly related to long-term motor learning, the fact that the neurons exhibiting plasticity were found in the behavioral plateau remains intriguing. Indeed, some indication suggests that the monkeys' behavior was not completely stationary even when the mean CC had reached the plateau. After completion of the present study, one of the monkeys was used for a follow-up experiment where the two force fields were presented within the same session (DiLorenzo, 1999). In that experiment, the results of which will be presented elsewhere, the monkey underwent the following sequence of epochs: Baseline, Force A, Washout, Force B, Washout, Force A, Washout. Force fields A and B were the same clockwise and counterclockwise force fields used here, with the order of presentation counterbalanced across sessions. Although the monkey was already familiar with both force fields, we observed that the performance in the second force field was generally worse than the performance in the first force field. In other words, the mean CC in the second force field was lower, independent of which force field was presented first (clockwise or counterclockwise). This interference would not be expected had the monkey learned both force fields so well that their corresponding internal models could be switched on and off at "no cost." Instead, this observation suggests that even in the plateau region of the long-term learning, the monkeys were still completing the development of the internal models for the force fields.

In the interpretation proposed, the neuronal plasticity reflects the development of an internal model of the movement dynamics. A distinct and complementary interpretation can also be considered. The changes of the tuning curves outlasting the dynamic adaptation might reflect the temporal "nonstationarity" of the cortex. In an always-changing environment, the nervous system constantly reorganizes itself to meet its needs. In the motor areas of the cerebral cortex, the reorganization occurs to accomplish the desired motor acts. While subsequent changes overwrite each other, any time the nervous system encounters a new environment, a subpopulation of neurons modify the activity to accommodate the new conditions. In this view, our observations are the fingerprints of a continuous reorganization of the nervous system, suggesting that neuronal plasticity is the rule rather than an exception.

Kinematic versus "Load" Modulation of M1 Neurons

Consistent with previous experiments, the present results provide evidence that the movement-related neuronal activity in primary motor cortex can be modulated by loads. Earlier work demonstrated that the discharge of many motor cortical cells varies with muscle activity (Evarts, 1968; Humphrey et al., 1970; Thach, 1978; Cheney and Fetz, 1980; Fromm, 1983). Neuronal activity increased when the monkey moved against an opposing

represented in red and lie on the *y* axis. The "*x-y-z*" cells are represented in gray. The arrows in (Aa) indicate the direction of the force field. The two monkeys (B and M) and the two force fields, clockwise (CK) and counterclockwise (CCK), are represented by the symbols: circles (B, CK), squares (B, CCK), triangles (M, CK), and diamonds (M, CCK).

Off-diagonal plots. The off-diagonal plots compare the classification of cells based upon different parameters. For each neuron, the position on the axes represents the changes of one parameter (axes), while the color represents the category based upon a different parameter (color). The conventions for colors are the same as for the diagonal plots. (Ab, top center) The axes refer to the changes of Pd (axes: Pd), while the colors refer to the changes of Avf (color: Avf). The neurons shown in plot (Ab) are the same neurons shown in plot (Aa). However, in plot (Ab), there is no systematic relationship between the position and the colors. In other words, there is no consistent correspondence between the classification based upon the two parameters Pd and Avf. (Ba, center left) further testifies the independence between the changes of Avf (axes: Avf) and the changes of Pd (color: Pd). Note that of the 137 neurons shown in plot (Bb), only 64 are present in plot (Ba); these 64 are the neurons that were significantly tuned in all three epochs and that could be classified according to the Pd. (Ac) (axes: Pd; color: Tw) and (Ca) (axes: Tw, color: Pd) illustrate the relations between the changes of Pd and the changes of Tw. (Bc) (axes: Avf; color: Tw) and (Cb) (axes: Tw, color: Avf) illustrate the relations between the changes of Avf and the changes of Tw. Only the 25 neurons that could be classified according to the Tw are shown in plots (Ac), (Ca), (Bc), and (Cb).

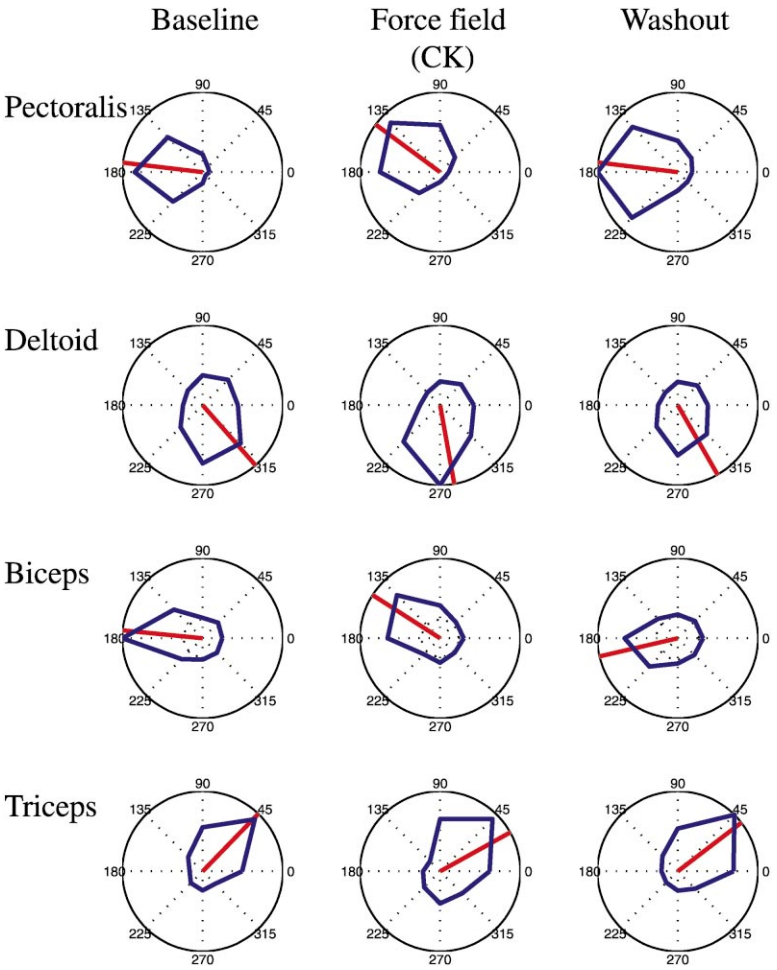

Figure 7. Muscles EMG

EMG activity recorded with a clockwise (CK) force field. The EMG activity was rectified and integrated over the same movement-related time window used for cells. For each muscle, the Pd shifts in the CK direction in the Force epoch, and in the CCK direction in the Washout.

load, and decreased when the load facilitated the movements. More recently, the responses of motor cortical neurons were systematically examined in monkeys performing center-out planar movements, compensating for a load that pulled the arm in eight different directions (Kalaska et al., 1989). The clockwise and counterclockwise curl forces used in our experiment imposed a load whose direction was always orthogonal to the direction of movement. The modulations of neuronal activity we obtained were therefore not readily comparable to those obtained by Kalaska and colleagues. A close examination of Figure 6 of that study, however, reveals that the preferred direction of that M1 neuron rotates in the direction of the force, similar to what we observed in the present work.

Though of a smaller proportion, we also found neurons that appeared to encode the direction of movement independently of changes in muscle activity. The percentage of kinematic cells obtained in the current study (9%–34%, depending on the parameter) is smaller than the 41% obtained in a study in which the direction of movement and muscle activity was dissociated using opposing and assisting torque load (Crutcher and Alexander, 1990), though comparable to that documented in other studies (Kalaska et al., 1989; Scott and Kalaska, 1997). More recently, in a behavioral task dissociating muscle activity, direction of joint movement, and direction of movement in space, it was demonstrated that muscle-like neuronal activity and activity that reflected the direction of joint movement in space coexisted in M1 (Kakei et al., 1999). The authors suggested that both "muscles" (28/88 neurons) and "movements" (44/88 neurons) are represented in the primary motor cortex. These results, together with those obtained in other studies (Georgopoulos et al., 1992; Shen and Alexander, 1997; Zhang et al., 1997), suggested that M1 harbors dynamic processes that translate stimulus representation into motor outputs.

In our statistical analysis, the kinematic category was always the null hypothesis. In other words, we classified cells based on *changes* of their parameters, and we included them in the class of kinematic cells if no changes were observed. Thus, no strong claims can be made regarding the functional role of kinematic cells. Furthermore, when multiple parameters were considered at the same time, the large majority of neurons showed some change across epochs. On the other hand, our task provided a strong constraint on the activity of muscles, namely a shift of the preferred direction. Indeed, the argument based on the vectorial summation of the force exerted by muscles and the force exerted by the manipulandum (illustrated in Figure 1D) would predict that the shift of preferred direction occurs for *any* muscle directionally tuned in the task. It is thus surprising that a relatively large population of cells does not show any shift of preferred direction across epochs

Table 2. Muscles

	Preferred Direction	Average Firing Rate	Tuning Width
Kinematic (*x-x-x*)	2 (17%)	4 (25%)	3 (30%)
Dynamic (*x-y-x*)	6 (50%)	2 (13%)	4 (40%)
Memory I (*x-y-y*)	1 (8%)	5 (31%)	2 (20%)
Memory II (*x-x-y*)	0	2 (13%)	0
Other (*x-y-z*)	3 (25%)	3 (19%)	1 (10%)
Total	12 (100%)	16 (100%)	10 (100%)

(kinematic cells, 34%). In this regard, it is also noteworthy that in the present study the monkeys were not only switching between different dynamic environments, but were also learning a new force field. The kinematic cells were thus not only noncorrelated with the dynamics of the movements, but also "resistant" to a motor learning experience.

Changes of Average Firing Frequency

Changes of neuronal activity across behavioral epochs occurred in the preferred direction (Pd), the average firing frequency (Avf), and the tuning width (Tw). At the population level, we noted a general increase of the Avf as the monkey performed across the three behavioral epochs. The fact that the Avf continued to increase in the Washout suggests that factors other than the load imposed by the external force should be considered. One possibility is that this increase is related to the adaptation process, similar to the shift of Pd. An alternative explanation, however, is that the monkeys became fatigued as they continued the task, such that more cortical output was required to generate muscle contractions adequate for movement. In a study in which the activity of motor cortex neurons was recorded in monkeys trained to perform self-paced isometric contractions, 50% (13/26) of the neurons increased and 31% (8/26) decreased in discharge frequency during muscle fatigue (Belhaj-Saif et al., 1996). Therefore, we cannot rule out the possibility that the change of Avf observed in the current study reflects, at least in part, fatigue of the cortico-motor circuitry.

Movement Speed

It has been proposed that the activity of M1 reflects movement speed (Moran and Schwartz, 1999). In the following, we explicitly address the issue of whether speed fluctuations can explain our observations and we conclude that they cannot.

Because the trajectories were essentially straight in all three epochs, we referred to a modified version of the model of Moran and Schwartz: $m(\vartheta) = v(\vartheta)\cos(\vartheta - \phi)$, where $m(\vartheta)$ was the firing rate of the cell and $v(\vartheta)$ was the speed. Thus, the tuning curve of cells was the product of a spatial, cosine-shaped tuning curve and a speed tuning curve $v(\vartheta)$. For each day, we computed the speed tuning curve in the three epochs. The speed profile was integrated from the movement onset to the end of movement, and the tuning curves were computed as was done for neurons.

To test for uniformity of distribution across directions, we first combined all the days, separately for the two force fields. We obtained six speed tuning curves (3 epochs $\times$ 2 force fields), none of which was significantly nonuniform (all $pR > 0.40$, Rayleigh test). Thus, the hypothesis that changes of neuronal Pd correlate with changes of speed can be rejected. Furthermore, it can be shown that, independently of the shape of $v(\vartheta)$, the homogeneous distribution of neuronal preferred directions in all three epochs is sufficient to exclude this hypothesis. We also performed a correlation analysis on a cell-by-cell basis. For each cell, we computed the corresponding speed tuning curve $v(\vartheta)$ and its Pd. Then we studied the correlation between changes of neuronal Pd and changes of the corresponding speed Pd, separately for each pair of epochs (Force-Baseline, Washout-Force, and Washout-Baseline). For a cell to participate in this analysis, we imposed the conditions of directional nonuniformity on both the neuronal and the speed tuning curves (condition $pR < 0.05$, Rayleigh test). When defined, the changes of speed Pd were essentially at random. Consistently, none of the three correlations was significant (all $r^2 < 2\%$). We conclude that changes of neuronal Pd do not correlate with fluctuations of speed.

To test for changes of average speed across epochs, we first combined the data of both monkeys and both force fields (91 days total). We found no changes in the Force compared to the Baseline (mean = 2%, $p = 0.13$), and a modest increase in the Washout compared to the Force (mean = 5%, $p = 0.03$). We then investigated on a cell-by-cell basis whether the change in neuronal Avf correlated with speed fluctuations. For each pair of epochs, we computed the correlation between the changes of neuronal Avf and the changes of average speed. None of these were significant (all $r^2 < 14\%$). We conclude that the changes of neuronal Avf do not correlate with fluctuations of speed.

As no instance satisfied both the conditions of directional nonuniformity and unimodality for both the neuronal and the speed tuning curve, the correlation could not be studied for the Tw.

Taken together, these results confirm that the kinematics were essentially constant throughout the task and that changes of neuronal activity across epochs reflect the change of movement dynamics and the adaptation to the force field.

Conclusions

In conclusion, we presented a paradigm that dissociates movement kinematics from movement dynamics and motor performance from the effects of motor adaptation. By choosing a specific, rotation invariant, dynamic perturbation, we were able to make stringent predictions on the effects of the perturbation on muscle activity. We then used the muscles as a framework to interpret the neuronal activity recorded from M1. We presented evidence of neuronal plasticity associated with dynamic adaptation and development of a new internal model. In response to the changing dynamics of the environment, neurons changed their firing rate and spatial tuning properties. Plastic changes outlasted the exposure to

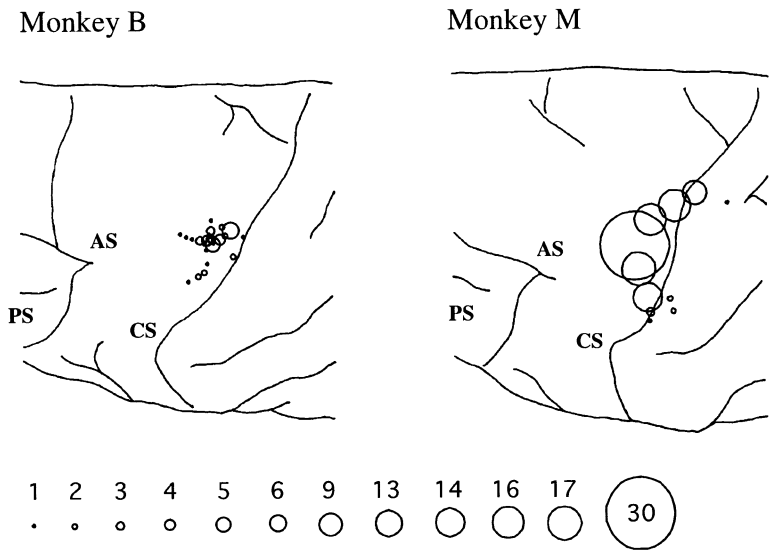

Figure 8. Gross Histology

Reconstruction of the recording sites on the surface of the brain for the two monkeys. The circles illustrate the number of cells recorded from the corresponding coordinates. CS, central sulcus; AS, arcuate sulcus; PS, principal sulcus.

the perturbation. Remarkably, changes of neuronal activity across behavioral conditions combined in a way adequate to support both functions of motor performance and motor learning.

Experimental Procedures

Behavioral Task

Two adult male macaque monkeys (*Macaca nemestrina*) were used in the experiment. Both monkeys performed with their right arm. The monkeys held a two-link low-friction manipulandum and performed the reaching task in an electrically isolated enclosure (Figure 1A). Two torque motors at the base of the manipulandum could apply perturbing force field upon the hand of the monkey. The monkeys forearm was positioned approximately parallel to the ground and the monkeys could move their arm freely during the task. Movements were confined to the horizontal plane. A computer monitor, situated 75 cm in front of the monkey and slightly below eye level, displayed the targets of the movement and a cursor representing the position of the manipulandum handle. The center square and peripheral targets were represented by squares of 14 by 14 mm (corresponding to ca 1° of visual angle) and the cursor by a square of 3 by 3 mm (ca 0.2° of visual angle).

The behavioral paradigm was a delayed, visually guided, reaching task (Figure 1B). A center square appeared in the center of the monitor before the beginning of each trial. The monkeys moved the cursor into the center square to initiate the trial. After 1,000 ms, a peripheral target appeared randomly at one of eight locations evenly spaced in a circle corresponding to 10 cm of actual distance in the center-out movement. The monkeys held the cursor within the center square for a variable period of 800 to 1,200 ms after the appearance of the peripheral target. The center square was then extinguished (the "GO" signal). The monkeys had to move and acquire the peripheral target within 1,200 ms after the "GO" signal appeared and remain within the peripheral target for another 1,000 ms to complete the task and receive a juice reward. During the movement, the trajectory had to be confined to an area subtended by an angle of 60° on both sides of the line connecting the center square and the peripheral target. Such a large spatial window was used to accommodate the possible perturbations of movements. The same time constraints and spatial windows were used for the three behavioral epochs. The trial was terminated if the monkeys made a mistake at any time during the task, and a new trial was initiated after a randomly selected inter-trial interval of 1 to 2 s.

In each session, the monkeys performed in three behavioral epochs (Baseline–no force; Force epoch–force field; Washout–no force), each with approximately 160 successful trials. The force fields used in the current experiments were vector fields $\mathbf{F} = \mathbf{BV}$, where **B** is a constant viscosity matrix and **V** is the instantaneous hand velocity vector in Cartesian coordinates (Shadmehr and Mussa-Ivaldi, 1994). For **B,** we chose an antidiagonal rotation matrix [0 b; −b 0] that defined a viscous, curl force field. The force field was viscous in that the magnitude of the applied forces was proportional to the instantaneous hand speed ($\|\mathbf{V}\|$) and curl in that the force direction was orthogonal to the instantaneous hand velocity (**V**). We chose $b = \pm 0.07$ N s/m. Depending on the sign, **F** was clockwise (CK, $b > 0$) or counterclockwise (CCK, $b < 0$).

The monkeys performed at an 80% success rate (in the Baseline epoch), after 4 to 6 months of training on the behavioral task. At no time during training were the monkeys exposed to the force fields used for recordings. Recording sessions using the two force fields were run in blocks, with each block occurring over a period of 1 to 5 months. The CK force field was studied first for both monkeys. The quality of the performance was quantified with a correlation coefficient (CC, see below). In each session, the CC showed an adaptation curve (Figure 2A). Over sessions, the adaptation became faster (shorter ramp) and better (higher asymptote). Monkey B underwent 40 sessions (CK) and 10 sessions (CCK) with the two force fields, respectively. The mean CC approximately reached plateau after 25 and 6 sessions, respectively. Monkey M underwent 25 sessions (CK) and 16 sessions (CCK) with the two force fields, respectively. The mean CC reached plateau after 15 and 8 sessions, respectively. During the sessions of the plateau region, the CC reached asymptote and the trajectories became straight within 30 trials in each epoch (C. Padoa-Schioppa et al., 1998, Soc. Neurosci., abstract).

Surgery, Recording, Electrical Microstimulation, and Animal Care

After training and under aseptic stereotaxic surgery, we implanted a restraint device on the skull and a recording well (18 mm, inner diameter) over the left primary motor cortex (M1). The location of M1 was verified by magnetic resonance imaging prior to surgery. The monkeys were given antibiotics and pain medications, and were allowed full rest for at least one week following the surgery. The NIH guidelines on the care and use of animals were strictly adhered to throughout the experiment.

Vinyl-coated tungsten electrodes (1–3 MΩ impedance) were used for recordings. Electrodes were advanced initially in the experiment through a hydraulic microdrive with a depth resolution of 1 μm and later by manually rotating a threaded rod carrying the electrode in a set-screw system at an approximate depth resolution of 30 μm (300 μm/turn). Up to three electrodes were used in each session. Electrical signals were passed through a head stage (AI 401, Axon Instruments) and an amplifier (Cyberamp 380, Axon Instruments) and filtered at a high and low cutoff of 10K Hz and 300 Hz, respec-

tively. Action potentials were detected by threshold crossing and waveforms (1.75 ms duration, 25 kHz) were recorded (Experimenter's WorkBench 5.1, DataWave Technology) and digitized for subsequent clustering.

Electrical microstimulations were performed in separate sessions to verify the recording locations. A train of 20 biphasic charge balanced pulse pairs (pulse width = 0.1 ms, train duration = 60 ms) was delivered at 330 Hz. At most sites, muscle twitches in the shoulder and forearm were elicited with a current magnitude of 20 μ Amp.

We manually implanted teflon-insulated wires into the pectoralis, deltoid, biceps, triceps, and brachioradialis muscles in separate sessions. The electromyographic (EMG) activity was recorded, rectified, and integrated over the movement-related time window. The response magnitudes were normalized and submitted to the same analyses used for cells. Sixteen instances of muscles were considered in the final sample (three pectoralis, five deltoid, four biceps, two triceps, and two brachioradialis).

Both monkeys were euthanized at the end of the experiment. They were given an overdose of pentobarbital sodium and then perfused transcardially with heparinized saline, followed by buffered Formalin. The brain was removed from the skull following standard procedures. Examination of the penetration marks on the surface of the brain revealed that they were primarily concentrated on the anterior bank of the central sulcus, at a location corresponding to the arm area of the primary motor cortex (Figure 8).

Data Analysis

The correlation coefficient (CC) was defined as in human studies. Briefly, from each trajectory ($x(t)$, $y(t)$), we extracted the speed profile $\mathbf{v} = (\dot{x}^2(t) + \dot{y}^2(t))^{1/2}$. We then derived an ideal speed profile $\mathbf{u}$ through an iterative process through all trials in the Baseline. The vectors $\mathbf{v}$ and $\mathbf{u}$ were aligned at their maximum and the CC was defined as the normalized covariance of $\mathbf{v}$ and $\mathbf{u}$ (see Shadmehr and Mussa-Ivaldi, 1994 for details):

$$CC\ (\mathbf{v},\mathbf{u}) = \frac{cov(\mathbf{v},\mathbf{u})}{\sigma(\mathbf{v})\sigma(\mathbf{u})}$$

In essence, the CC quantifies the similarity between the actual and the ideal speed profiles.

Individual neurons recorded from the same electrode were first separated through manual clustering. Only cells whose waveform was convincingly consistent throughout the recordings (as valued by visual inspection) were considered for further analysis.

All the results on the neuronal and muscular activity refer to the same movement-related time period (from 200 ms before the movement onset to the end of the movement). The onset and termination of the movement were defined with a speed threshold criterion (4 cm/s) during the acceleration and deceleration phase of the movement.

In each session, we arbitrarily considered that the monkeys had reached the steady-state region after they had performed four successful trials in each direction of movement. Only the remaining trials were considered for further analysis.

The activity of each neuron was separately analyzed in the Baseline, Force field, and Washout epochs. For each epoch and for each direction, we considered the mean activity across trials. We obtained three tuning curves and we defined the preferred direction (Pd), average firing rate (Avf), and tuning width (Tw). Pd was as the direction of the vector average of the tuning curve. Avf was the average of the tuning curve. Tw was the angle over which the firing frequency was higher than half the maximum of the tuning curve. The Tw was not defined for multimodal cells, for which the directions with firing frequency higher than half the maximum were noncontinuous.

Our analysis focused on cells with Avf $>$ 1 Hz. Of the 162 neurons considered, 137 neurons satisfied this criterion in all three behavioral epochs. Sixty-four neurons had a significantly nonuniform activity across the eight directions in all three epochs (Rayleigh test, pR $<$ 0.05). Twenty-five neurons were unimodal in all three epochs.

The neuronal recordings were carried out over several months. No effort was made to locate the cortical layer of the recording sites. Thus, we cannot ascertain whether the different classes of neurons were segregated in different cortical layers. However, different classes of neurons were recorded in the same locations on the surface and sometimes even from the same electrode (i.e., at the same time).

Because our results rest upon the changes observed in tuning curves, several concerns were considered. In general, since the change of Pd of neurons was consistently in the direction of the perturbing force, random sources of noise can hardly account for the alterations of neuronal activity. In addition, we analyzed only neurons with excellent recording stability, addressing the concern of poor isolation. Finally, monkeys adopted a stable body position and a stereotypical arm configuration while performing the task, suggesting that the changes of neuronal activity did not reflect postural changes (Scott and Kalaska, 1995, 1997; Sergio and Kalaska, 1997).

Statistical Analysis of Tuning Curves

We statistically compare the three parameters (Pd, Avf, and Tw) across epochs using the following method. In each epoch, we repeatedly measure the firing rate t_i of the cell for movements in the direction i, and $i = 1,...8$. We indicate with $t_i(j)$ the j^{th} measure of t_i, and we have $j = 1...n_i$ and $n_i \approx 20$. t_i is a random variable with expectation value μ_i and finite variance $Var(t_i)$. If μ_i is the expected firing rate of the cell for movements in direction i, a parameter is a function:

$$p = P(\mu_i) \tag{1}$$

and we want to compare values of p obtained in different epochs. The best estimate we have for μ_i is:

$$m_i = \frac{1}{n_i}\sum_{j=1}^{n_i} t_i(j) \tag{2}$$

namely the average of many measures of the firing rate t_i. The variance $Var(t_i)$ can be estimated through:

$$Var(t_i) \approx s_i^2 = \frac{1}{n_i - 1}\sum_{j=1}^{n_i} (t_i(j) - m_i)^2 \tag{3}$$

For high values of n_i ($n_i \approx 20$ in our case), m_i can be safely treated as a Gaussian variable $m_i{:}N(\mu,\sigma_i^2)$. Furthermore, because a liner combination $f = ax + by + c$ of Gaussian variables $x{:}N(\mu,\sigma^2)$ and $y{:}N(\mu,\sigma^2)$ is itself a Gaussian variable with $f{:}N((a + b)\ \mu + c, (a^2 + b^2)\sigma^2)$ (Devore, 1990, p.212), we have: $\sigma_i^2 = Var(t_i)/n_i$. Thus, we can consider m_i as a measure of μ_i affected by a square error σ_i^2. Note that while the expectation value of s_i^2 is $Var(t_i)$, independent of the number of measures n_i, the expectation value of σ_i^2 is $Var(t_i)/n_i$, a decreasing function of n_i.

The idea of the method is to propagate to the parameter p the error of measure σ_i^2 of μ_i. We develop the parameter $p = P(\mu_i)$ close to μ_i at the first order in $(m_i - \mu_i)$:

$$P(m_i) \approx P(\mu_i) + \sum_i \left.\frac{\partial P}{\partial m_i}\right|_{\mu} (m_i - \mu_i) \tag{4}$$

This approximation is best for smooth functions $P(m_i)$, and for small values of $|m_i - \mu_i|$. The expectation value of $|m_i - \mu_i|$ is σ_i^2, which is smaller for higher n_i. Following Equation (4), p is Gaussian, with:

$$p : N\left(P(\mu_i), \sum_i \left(\left.\frac{\partial P}{\partial m_i}\right|_{\mu}\right)^2 \sigma_i^2\right) \equiv N(P(\mu_i), \sigma_p^2) \tag{5}$$

We are left with the problem of comparing two Gaussian variables, for which we have the measures of the mean values and the estimates of the variances. This can be done with a conventional z test.

The cells presented in this paper were classified by running three z tests. We obtained three p values for the three pairs of epochs (p_{fb} for Force-Baseline, p_{wf} for Washout-Force, p_{wb} for Washout-Baseline). Cells were classified as kinematic, dynamic, or memory for a given parameter by setting a threshold $\alpha = 0.05$, below which we rejected the null hypothesis. For instance, we classified as dynamic a cell with $p_{fb} < \alpha$, $p_{wf} < \alpha$, $p_{wb} > \alpha$. Analogously, we did for the other categories of cells. We also had some dubious cases, for

instance when $p_{fb} < \alpha$, $p_{wf} > \alpha$, $p_{wb} > \alpha$. The first p value indicates an activity in the Force epoch different than the one in the Baseline, but neither of the differences between Washout-Force and Washout-Baseline is significant. We proceeded in this case according to the lowest p value, so that we classified the cell as dynamic if $p_{wf} < p_{wb}$, and as memory if $p_{wf} > p_{wb}$.

Acknowledgments

We thank Brian Benda for participating at an early stage of the present work and Dan DiLorenzo for helping us with the EMG recordings. We are also thankful to Matt Tresch, Andrea d'Avella, Philippe Saltiel, and Emanuel Todorov for helpful discussions and to Lori Markson for editing the manuscript. This study was supported by the NIH grant number MN481185.

Received November 27, 2000; revised February 20, 2001.

References

Aosaki, T., Tsubokawa, H., Ishida, A., Watanabe, K., Graybiel, A.M., and Kimura, M. (1994). Responses of tonically active neurons in the primate's striatum undergo systematic changes during behavioral sensorimotor conditioning. J. Neurosci. *14*, 3969–3984.

Belhaj-Saif, A., Fourment, A., and Maton, B. (1996). Adaptation of the precentral cortical command to elbow muscle fatigue. Exp. Brain Res. *111*, 405–416.

Borsook, D., Becerra, L., Fishman, S., Edwards, A., Jennings, C.L., Stojanovic, M., Rapinicolas, L., Ramachandran, V.S., Gonzalez, R.G., and Breiter, H. (1998). Acute plasticity in the human somatosensory cortex following amputation. Neuroreport *9*, 1013–1017.

Chen, L.L., and Wise, S.P. (1995). Neuronal activity in the supplementary eye field during acquisition of conditional oculomotor associations. J. Neurophysiol. *73*, 1101–1121.

Cheney, P.D., and Fetz, E.E. (1980). Functional classes of primate corticomotoneuronal cells and their relation to active force. J. Neurophysiol. *44*, 773–791.

Classen, J., Liepert, J., Wise, S.P., Hallett, M., and Cohen, L.G. (1998). Rapid plasticity of human cortical movement representation induced by practice. J. Neurophysiol. *79*, 1117–1123.

Crutcher, M.D., and Alexander, G.E. (1990). Movement-related neuronal activity selectively coding either direction or muscle pattern in three motor areas of the monkey. J. Neurophysiol. *64*, 151–163.

Devore, J.L. (1990). Probability and Statistics for Engineering and Sciences (Pacific Grove, CA: Brooks/Cole).

DiLorenzo, D.J. (1999). Correlates of motor performance in the primary motor cortex, PhD thesis, Massachusetts Institute of Technology, Cambridge, Massachusetts.

Dinse, H.R., Godde, B., Hilger, T., Haupt, S.S., Spengler, F., and Zepka, R. (1997). Short-term functional plasticity of cortical and thalamic sensory representations and its implication for information processing. Adv. Neurol. *73*, 159–178.

Donoghue, J.P. (1995). Plasticity of adult sensorimotor representations. Curr. Opin. Neurobiol. *5*, 749–754.

Dorris, M.C., Pare, M., and Munoz, D.P. (2000). Immediate neural plasticity shapes motor performance. J. Neurosci. *20*, RC52.

Elbert, T., Pantev, C., Wienbruch, C., Rockstroh, B., and Taub, E. (1995). Increased cortical representation of the fingers of the left hand in string players. Science *270*, 305–307.

Evarts, E.V. (1968). Relation of pyramidal tract activity to force exerted during voluntary movement. J. Neurophysiol. *31*, 14–27.

Faggin, B.M., Nguyen, K.T., and Nicolelis, M.A. (1997). Immediate and simultaneous sensory reorganization at cortical and subcortical levels of the somatosensory system. Proc. Natl. Acad. Sci. USA *94*, 9428–9433.

Fisher, N.I. (1993). Statistical Analysis of Circular Data (Cambridge University Press).

Florence, S.L., and Kaas, J.H. (1995). Large-scale reorganization at multiple levels of the somatosensory pathway follows therapeutic amputation of the hand in monkeys. J. Neurosci. *15*, 8083–8095.

Fromm, C. (1983). Changes of steady state activity in motor cortex consistent with the length-tension relation of muscle. Pfluegers Arch. *398*, 318–323.

Gandolfo, F., Li, C.-S.R., Benda, B., Padoa-Schioppa, C., and Bizzi, E. (2000). Cortical correlates of motor learning in monkeys adapting to a new dynamic environment. Proc. Natl. Acad. Sci. USA *97*, 2259–2263.

Georgopoulos, A.P., Ashe, J., Smyrnis, N., and Taira, M. (1992). The motor cortex and the coding of force. Science *256*, 1692–1695.

Hess, G., Aizenman, C.D., and Donoghue, J.P. (1996). Conditions for the induction of long-term potentiation in layer II/III horizontal connections of the rat motor cortex. J. Neurophysiol. *75*, 1765–1778.

Hikosaka, O., Sakai, K., Nakahara, H., Lu, X., Miyachi, S., Nakamura, K., and Rand, M.K. (2000). Neural mechanisms for learning of sequential procedures. In the New Cognitive Neurosciences, M.S Gazzaniga, ed. (Cambridge, MA: MIT Press), pp 553–572.

Humphrey, D.R., Schmidt, E.M., and Thompson, W.D. (1970). Predicting measures of motor performance from multiple cortical spike trains. Science *179*, 758–762.

Huntley, G.W. (1997). Correlation between patterns of horizontal connectivity and the extend of short-term representational plasticity in rat motor cortex. Cereb. Cortex *7*, 143–156.

Kakei, S., Hoffman, D.S., and Strick, P.L. (1999). Muscle and movement representations in the primary motor cortex. Science *285*, 2136–2139.

Kalaska, J.F., Cohen, D.A., Hyde, M.L., and Prud'homme, M. (1989). A comparison of movement direction-related versus load direction-related activity in primate motor cortex, using a two-dimensional reaching task. J. Neurosci. *9*, 2080–2102.

Karni, A., Meyer, G., Jezzard, P., Adams, M.M., Turner, R., and Ungerleider, L.G. (1995). Functional MRI evidence for adult motor cortex plasticity during motor skill learning. Nature *377*, 155–158.

Laubach, M., Wessberg, J., and Nicolelis, M.A. (2000). Cortical ensemble activity increasingly predicts behaviour outcomes during learning of a motor task. Nature *40*, 567–571.

Manger, P.R., Woods, T.M., and Jones, E.G. (1996). Plasticity of the somatosensory cortical map in macaque monkeys after chronic partial amputation of a digit. Proc. Royal Soc. London *263*, 933–939.

Mitz, A.R., Godschalk, M., and Wise, S.P. (1991). Learning-dependent neuronal activity in the premotor cortex: activity during the acquisition of conditional motor associations. J. Neurosci. *11*, 1855–1872.

Moran, D.W., and Schwartz, A.B. (1999). Motor cortical representation of speed and direction during reaching. J. Neurophysiol. *82*, 2676–2692.

Nakamura, K., Sakai, K., and Hikosaka, O. (1998). Neuronal activity in medial frontal cortex during learning of sequential procedures. J. Neurophysiol. *80*, 2671–2687.

Nudo, R.J., Milliken, G.W., Jenkins, W.M., and Merzenich, M.M. (1996). Use-dependent alterations of movement representations in primary motor cortex of adult squirrel monkeys. J. Neurosci. *16*, 785–807.

Pascual-Leone, A., Grafman, J., and Hallett, M. (1994). Modulation of cortical motor output maps during development of implicit and explicit knowledge. Science *263*, 1287–1289.

Recanzone, G.H., Schreiner, C.E., and Merzenich, M.M. (1993). Plasticity in the frequency representation of primary auditory cortex following discrimination training in adult owl monkeys. J. Neurosci. *13*, 87–103.

Sakai, K., and Miyashita, Y. (1991). Neural organization for the long-term memory of paired associates. Nature *354*, 152–155.

Scott, S.H., and Kalaska, J.F. (1995). Changes in motor cortex activity during reaching movements with similar hand paths but different arm postures. J. Neurophysiol. *73*, 2563–2567.

Scott, S.H., and Kalaska, J.F. (1997). Reaching movements with similar hand paths but different arm orientations. I. Activity of individual cells in motor cortex. J. Neurophysiol. *77*, 826–852.

Sergio, L.E., and Kalaska, J.F. (1997). Systematic changes in directional tuning of motor cortex cell activity with hand location in the

workspace during generation of static isometric forces in constant spatial directions. J. Neurophysiol. *78*, 1170–1174.

Shadmehr, R., and Mussa-Ivaldi, F.A. (1994). Adaptive representation of dynamics during learning of a motor task. J. Neurosci. *14*, 3208–3224.

Shen, L., and Alexander, G.E. (1997). Neural correlates of a spatial sensory-to-motor transformation in primary motor cortex. J. Neurophysiol. *77*, 1171–1194.

Thach, W.T. (1978). Correlation of neural discharge with pattern and force of muscular activity, joint position, and direction of intended next movement in motor cortex and cerebellum. J. Neurophysiol. *41*, 654–676.

Thoroughman, K.A., and Shadmehr, R. (1999). Electromyographic correlates of learning an internal model of reaching movements. J. Neurosci. *19*, 8573–8588.

Wise, S.P., Moody, S.L., Blomstrom, K.J., and Mitz, A.R. (1998). Changes in motor cortical activity during visuomotor adaptation. Exp. Brain Res. *121*, 285–299.

Xerri, C., Merzenich, M.M., Peterson, B.E., and Jenkins, W. (1998). Plasticity of primary somatosensory cortex paralleling sensorimotor skill recovery from stroke in adult monkeys. J. Neurophysiol. *79*, 2119–2148.

Zhang, J., Riehle, A., Requin, J., and Kornblum, S. (1997). Dynamics of single neuron activity in monkey primary motor cortex related to sensorimotor transformation. J. Neurosci. *17*, 2227–2246.